

## THE ANALYSIS OF SEISMIC STRESS REGIME IN AHAR- VARZEGHAN REGION, NORTHWESTERN IRAN

Mahsa AFRA

*MSc Student of Geophysics, Institute of Geophysics, University of Tehran, Tehran, Iran  
m\_afra006@ut.ac.ir*

Ali MORADI

*Assistant Professor, Institute of Geophysics, University of Tehran, Tehran, Iran  
asmoradi@ut.ac.ir*

Mehrdad PAKZAD

*Assistant Professor, Institute of Geophysics, University of Tehran, Tehran, Iran  
pakzad@ut.ac.ir*

**Keywords:** Stress, Focal Mechanism, ISOLA, Multiple Inverse Method, Ahar-Varzeghan

### ABSTRACT

We analyze stress state in northwestern Iran which includes Ahar-Varzeghan region by determining the focal mechanisms of 15 earthquakes using the moment tensor inversion method of ISOLA and also by focal mechanisms of other large and moderate earthquakes determined by GCMT. The events have moment magnitudes higher than 4 and encompass latitudes between 34- 40° N, and longitudes between 43- 51° E, during the period 1976-2013. We calculate the principal orientations of stresses in the region by multiple inverse method. The result shows the stress model with  $\sigma_1$  direction equal to 136.7 degree. In contrast, the direction of the principal stress is almost north-south in eastern Anatolia and east-west in western Caspian sea. This difference in geodynamic regimes in the study area may be attributed to the north Tabriz fault.

### INTRODUCTION

Northwestern Iran is one of the seismically active regions with a high seismic risk in the world endorsed by historical background and instrumental earthquakes. This area is part of the complex tectonic system due to the interaction between Arabia, Anatolia and Eurasia and comprises the North Anatolian Fault, the East Anatolian Fault, the Caucasus Mountains, and the Main Recent Fault which bounds the Zagros Mountains.

Our knowledge of stress state in a region is useful for a better understanding of different rupture mechanism. Stress is the main cause of earthquake and studying the present day stress regime in the crust is very important for understanding the current deformation in each area and specially in this region considering its dense population. The focal mechanism of an earthquake is one of the important source parameters which is needed for studying stresses and their variations as well as analyzing stress field. Using Earthquake focal mechanisms could help us investigate the stress regime. The big advantage of the focal mechanism solutions is the ability to study the stress regime at depth in the lithosphere. By inversion of all the available solutions we determine the best fitted reduced stress tensor by grouping focal mechanisms.

## DATA AND PROCEDURE

We use ISOLA software for moment tensor inversion in time domain using waveform modelling to determine focal mechanisms. The method was first offered to calculate the source parameters at teleseismic distances (Kikuchi and Kanamori, 1991). It was developed later for regional and local distances by Zahradnik et al. (2005). In this method, Green's functions are calculated by discrete wave number method (Bouchon, 1981). We used the broadband stations of Iranian Seismological Center (IRSC), International Institute of Earthquake Engineering and Seismology (IIEES) and also stations of several other countries bordering - northwestern Iran (table 1). We employ the 5- layer crustal model of IRSC shown in table 2 and determine the source parameters of 15 earthquakes by waveform modelling (table 3).

Table 1. Positions of used stations in this study

| Station | Lat (N °) | Long (E °) | Seismic Network |
|---------|-----------|------------|-----------------|
| BZA     | 34.4696   | 47.8605    | IGUT-IRSC       |
| DOB     | 33.78744  | 48.17747   | IGUT-IRSC       |
| HAGD    | 34.822    | 49.139037  | IGUT-IRSC       |
| HSRG    | 35.2418   | 48.2787    | IGUT-IRSC       |
| KCHF    | 34.275    | 47.0404    | IGUT-IRSC       |
| KFM     | 33.52444  | 47.84694   | IGUT-IRSC       |
| KMR     | 33.5178   | 48.3803    | IGUT-IRSC       |
| KOM     | 34.1761   | 47.5144    | IGUT-IRSC       |
| QABG    | 35.70846  | 49.58238   | IGUT-IRSC       |
| QALM    | 36.4321   | 50.64646   | IGUT-IRSC       |
| MAHB    | 36.7666   | 45.7054    | IGUT-IRSC       |
| TABZ    | 38.0568   | 46.3266    | IGUT-IRSC       |
| TAHR    | 38.49     | 47.051     | IGUT-IRSC       |
| TVRZ    | 38.504    | 46.668     | IGUT-IRSC       |
| ZNGN    | 32.1174   | 50.8542    | IGUT-IRSC       |
| ASAO    | 34.548    | 50.025     | IIEES-BIN       |
| CHTH    | 35.908    | 51.126     | IIEES-BIN       |
| GHVR    | 34.48     | 51.295     | IIEES-BIN       |
| GRMI    | 38.81     | 47.894     | IIEES-BIN       |
| KHMZ    | 33.739    | 49.959     | IIEES-BIN       |
| MAKU    | 39.355    | 44.683     | IIEES-BIN       |
| SNGE    | 35.093    | 47.347     | IIEES-BIN       |
| THKV    | 35.916    | 50.879     | IIEES-BIN       |
| ZNJK    | 36.67     | 48.685     | IIEES-BIN       |
| AGRB    | 39.5755   | 42.992     | GFZ             |
| GNI     | 40.149    | 44.7414    | GFZ             |
| KARS    | 40.6276   | 43.0788    | GFZ             |
| SIRT    | 37.5011   | 42.4392    | GFZ             |
| VANB    | 38.595    | 43.389     | GFZ             |

Table 2. Crustal model of Iran (IRSC)

| Depth of layer top (km) | Vp (km/s) | Vs (km/s) | Density (g/Cm3) | Qp  | Qs  |
|-------------------------|-----------|-----------|-----------------|-----|-----|
| 0.0                     | 5.38      | 3.057     | 2.776           | 600 | 300 |
| 7.0                     | 5.95      | 3.381     | 2.890           | 600 | 300 |
| 12.0                    | 6.15      | 3.494     | 2.930           | 600 | 300 |
| 20.0                    | 6.42      | 3.648     | 2.984           | 600 | 300 |
| 47.0                    | 8.06      | 4.580     | 3.312           | 600 | 300 |



Table 3. Determined focal mechanisms in this study

| NO. | Origin Time & Location Parameters |          |               |                |            |     | DC % | variance reduction % | Nodal Planes |         |          |
|-----|-----------------------------------|----------|---------------|----------------|------------|-----|------|----------------------|--------------|---------|----------|
|     | Date                              | Time     | Latitude (°N) | Longitude (°E) | Depth (Km) | MW  |      |                      | strike (°)   | dip (°) | rake (°) |
| 1   | 20120811                          | 12:23:15 | 38.43         | 46.81          | 6          | 6.4 | 67.0 | 80                   | 84           | 90      | 138      |
|     |                                   |          |               |                |            |     |      |                      | 174          | 48      | 0        |
| 2   | 20120811                          | 12:34:33 | 38.46         | 46.84          | 16         | 6.3 | 65.7 | 80                   | 81           | 87      | -175     |
|     |                                   |          |               |                |            |     |      |                      | 351          | 85      | -3       |
| 3   | 20120811                          | 15:21:14 | 38.42         | 46.8           | 6          | 4.8 | 82.9 | 50                   | 86           | 84      | -176     |
|     |                                   |          |               |                |            |     |      |                      | 355          | 86      | -6       |
| 4   | 20120811                          | 15:43:19 | 38.46         | 46.73          | 10         | 4.8 | 85.4 | 50                   | 31           | 67      | 69       |
|     |                                   |          |               |                |            |     |      |                      | 255          | 31      | 130      |
| 5   | 20120811                          | 22:24:02 | 38.43         | 46.75          | 10         | 5.3 | 77.7 | 60                   | 352          | 64      | 9        |
|     |                                   |          |               |                |            |     |      |                      | 258          | 82      | 154      |
| 6   | 20120813                          | 1:56:10  | 38.47         | 46.66          | 10         | 4.7 | 91.3 | 60                   | 266          | 90      | -175     |
|     |                                   |          |               |                |            |     |      |                      | 176          | 85      | 0        |
| 7   | 20120819                          | 1:58:30  | 38.41         | 46.65          | 10         | 4.3 | 61.7 | 60                   | 82           | 88      | 174      |
|     |                                   |          |               |                |            |     |      |                      | 172          | 84      | 2        |
| 8   | 20121027                          | 3:56:41  | 38.39         | 46.64          | 8          | 4.3 | 61.4 | 50                   | 83           | 71      | 166      |
|     |                                   |          |               |                |            |     |      |                      | 178          | 77      | 20       |
| 9   | 20121107                          | 6:26:31  | 38.46         | 46.75          | 10         | 5.8 | 75.1 | 80                   | 271          | 82      | -174     |
|     |                                   |          |               |                |            |     |      |                      | 180          | 84      | -8       |
| 10  | 20121116                          | 3:58:28  | 38.49         | 46.66          | 6          | 4.9 | 95.7 | 50                   | 280          | 81      | -169     |
|     |                                   |          |               |                |            |     |      |                      | 188          | 79      | -9       |
| 11  | 20121223                          | 6:38:57  | 38.48         | 44.93          | 14         | 5.2 | 91.6 | 70                   | 76           | 82      | 174      |
|     |                                   |          |               |                |            |     |      |                      | 167          | 84      | 8        |
| 12  | 20121223                          | 7:12:31  | 38.41         | 44.84          | 20         | 4.1 | 64.3 | 80                   | 83           | 61      | 147      |
|     |                                   |          |               |                |            |     |      |                      | 190          | 62      | 34       |
| 13  | 20130706                          | 17:07:49 | 37.63         | 48.96          | 10         | 4.0 | 77.7 | 60                   | 97           | 90      | -175     |
|     |                                   |          |               |                |            |     |      |                      | 7            | 85      | 0        |
| 14  | 20130927                          | 10:02:43 | 37.33         | 44.94          | 18         | 4.4 | 65.8 | 70                   | 75           | 59      | 107      |
|     |                                   |          |               |                |            |     |      |                      | 224          | 35      | 64       |
| 15  | 20131108                          | 10:12:34 | 37.8          | 47.17          | 6          | 4.4 | 96.0 | 70                   | 21           | 67      | -10      |
|     |                                   |          |               |                |            |     |      |                      | 115          | 81      | -157     |

The acquired and GCMT focal mechanisms are shown in figure 1, respectively in blue and red. Using the information of these events containing strike, dip and rake angles, we study the state of stress in the region. For this purpose, we use multiple inverse method that was originally proposed by Yamaji (2000). The method is a numerical technique to separate stresses from heterogeneous fault– slip and focal mechanism data. The method employs the inversion of earthquake focal mechanism to determine the principal stress orientations. The regions of azimuth and plunge of principal stresses;  $\sigma_1$  and  $\sigma_3$ , and also stress ratio for the specified regions are depicted by blue lines in figure 1, and numbered in table 4. The green arrows present the direction of principal stress;  $\sigma_1$ , in each specified region.

Stress ratio is defined as a ratio between the principal stress differences and expressed as Eq. 1.

$$\varphi = \frac{\sigma_2 - \sigma_3}{\sigma_1 - \sigma_3} \quad (1)$$

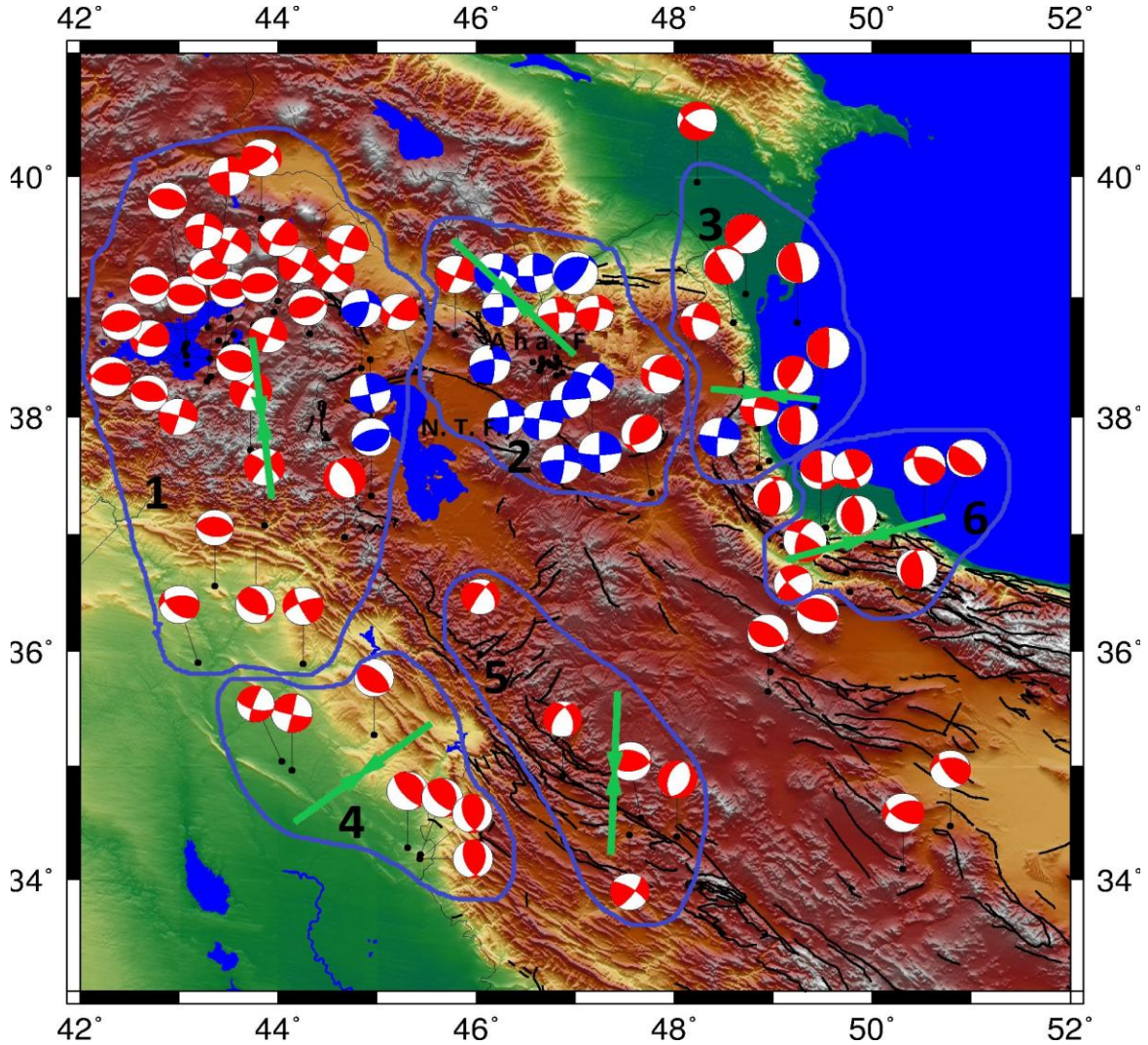


Figure 1. Determined focal mechanisms in this study (blue) during the period 2012-2013 and by GCMT (red) during the period 1976-2013. The blue lines present determined regions of different stress states in this study. The green arrows depict the directions of principal stress,  $\sigma_1$ , in each region.

Table 4. Calculated azimuth and plunge of principal stresses,  $\sigma_1$ ,  $\sigma_3$  and also stress ratio in each specified region of figure 1.

| Region | Azimuth $\sigma_1$ | Plunge $\sigma_1$ | Azimuth $\sigma_3$ | Plunge $\sigma_3$ | stress ratio |
|--------|--------------------|-------------------|--------------------|-------------------|--------------|
| 1      | 173.6              | 4.7               | 60.3               | 78.2              | 0.27         |
| 2      | 136.7              | 0.1               | 46.7               | 4.8               | 0.34         |
| 3      | 96.1               | 51.4              | 256.6              | 37                | 0.18         |
| 4      | 53.1               | 3.2               | 315                | 68.1              | 0.26         |
| 5      | 182.4              | 0.6               | 272.6              | 13.8              | 0.64         |
| 6      | 74.1               | 17                | 191.8              | 56.7              | 0.34         |

## CONCLUSIONS

As it is presented in figure 1 and table 4, the stress regime in Ahar-Varzeghan region is completely different from other surrounding areas. Most of the focal mechanisms are right lateral strike-slip and the direction of principal stress,  $\sigma_1$ , is  $136.7^\circ$ . Zagros, Alborz and Talesh mountains have different geodynamic regimes. Toward the west and in eastern Anatolia, the direction of principal stress,  $\sigma_1$ , is almost north-south. In contrast, the direction of this principal stress changes to east-west in western Caspian Sea. This difference in geodynamic regimes in the study area with the surrounding regions may be attributed to the north Tabriz fault.

## REFERENCES

- Bouchon M (1981) A Simple Method to Calculation Green's Function for Elastic Layered Media, *Bulletin of the Seismological Society of America*, 71: 959-971
- Otsubo M, Yamaji A and Kubo A (2008) Determination of Stresses from Heterogeneous Focal Mechanism Data: An adaptation of the multiple inverse method, *Tectonophysics*, 457: 150-160
- Sokos E and Zahradnic J (2008) ISOLA a Fortran Code and a Matlab GUI to Perform Multiple-Point Source Inversion of Seismic Data, *Computers and Geosciences*, 34: 967-977
- Yamaji A (2000b) The Multiple Inverse Method: a New Technique to Separate Stresses from Heterogeneous Fault-Slip Data, *Journal of Structural Geology*, 22: 441-452